Available online at www.sciencedirect.com
ScienceDirect
Journal of the European Ceramic Society 27 (2007) 1579–1584
www.elsevier.com/locate/jeurceramsoc

Crystallization of oxyapatite in glass-ceramics

Christian van't Hoen *, Volker Rheinberger, Wolfram Höland, Elke Apel

Ivoclar Vivadent AG, Bendererstr. 2, FL-9494 Schaan, Liechtenstein

Available online 30 May 2006

Abstract

The aim of the presented study was to investigate the crystallization of oxyapatites in glass-ceramics. The crystallization was analysed for three different glasses from the SiO_2–B_2O_3–Al_2O_3–Y_2O_3–CaO–Na_2O–K_2O–F system with different F and B_2O_3 content after heat treatment. To characterize the microstructure and the phase formation, we used scanning electron microscopy (SEM) and room temperature X-ray diffraction (RT-XRD). The main results of this study showed that the oxyapatite crystallization is different in comparison to that of fluorapatite. We detected that the oxyapatite crystallizes according to the surface crystallization mechanism. Also we determined leucite as a secondary crystal phase in dependence of the B_2O_3 and F content. The results showed that a two-fold controlled surface crystallization of oxyapatite and leucite took place.

Keywords: Apatite; Biomedical applications; Glass-ceramics; Silicate; Surface crystallization

1. Introduction

The development of glass-ceramics containing apatite crystals has been a focal point in the development of glass-ceramics for restorative dentistry as well as in research efforts conducted on the chemistry of bioactive glass-ceramics for the replacement of hard tissue. Initially, fluorapatite with the familiar hexagonal habit was produced in bioactive glass-ceramics (Brömer et al.[1] and Kokubo[2]). Subsequently, the discovery of needle-like apatite in bioactive glass-ceramics or glass-ceramics for dental restoration was made (Höland et al.,[3] Clifford and Hill[4] and Moisescu et al.[5]). These needle-shaped crystals are always produced according to the mechanism of controlled volume nucleation. The structural units of phosphate, which form spherical phases in the silicate glass matrix during phase separation processes, are the driving force of this reaction. In addition to glass-ceramics, Kolitsch et al.[6] developed sintered ceramics with oxyapatite crystals and Ito[7] described different types of silicate apatites and oxyapatites.

A typical glass formation system used in the development of leucite–apatite glass-ceramics for dental restorations is characterized by the following main components: SiO_2–Al_2O_3–K_2O–Na_2O–CaO–P_2O_5–F. The nucleation promoting effect of the phosphate structural units causes Ca^{2+} and F^- to concentrate in the spherical glass phase and initially, very small apatite crystals are formed. In the growth process, preferably at approximately 1000 °C (Höland and Beall,[8] Müller et al.[9] and van't Hoen et al.[10]) needle-like crystals grow according to the Ostwald ripening mechanism. These crystals can grow to a length of 10 μm.

The aim of the present study, however, was to control the precipitation of apatite in a phosphate-free glass formation system for dental restoration. The SiO_2–B_2O_3–Al_2O_3–Y_2O_3–CaO–Na_2O–K_2O–F base system was used for this purpose. Three compositions with different content of B_2O_3 and F were investigated. The goal of controlling the formation of oxyapatite, that is, ensuring a uniform crystal size and distribution in the glass matrix was pursued by controlling the heat treatment only (*in situ* process). The controlling mechanisms of nucleation and crystallization established in this study are discussed and initial conclusions on their quantification are also drawn.

2. Experimental

2.1. Chemical compositions

For the investigations of the precipitation of apatites in phosphate-free glasses we used three different multi-component compositions in the system SiO_2–B_2O_3–Al_2O_3–Y_2O_3–CaO–Na_2O–K_2O–F.

The chemical composition is very important to make exact conclusions on the results of this study. So we used different

* Corresponding author. Tel.: +423 235 3294; fax: +423 239 4294.
E-mail address: christian.vanthoen@ivoclarvivadent.com (C. van't Hoen).

0955-2219/$ – see front matter © 2006 Elsevier Ltd. All rights reserved.
doi:10.1016/j.jeurceramsoc.2006.04.095

methods to analyse the chemical composition of the investigated glasses.

2.2. Sample preparation (glasses and glass-ceramics)

Homogenous glasses were prepared using synthetic raw materials: silicon oxide, potassium carbonate, sodium carbonate, sodium fluoride, calcium carbonate, yttrium oxide, aluminium oxyhydroxyhydrate and boronoxide hydrate. For the first preliminary tests, monolithic glass blocks were also fabricated. The blocks were produced by casting the glass melt in a graphite crucible and subsequently annealing the material down to <250 °C.

The main research was carried out using glass powders. Therefore, the glasses were melted at 1550 °C for 2 h and subsequently quenched in cold water to produce a glass frit. The glass frits produced in this way were ground to powders featuring a grain size of <90 μm.

In a preliminary test, the monolithic samples were heat treated at different temperatures from 800 °C to 1000 °C with steps of 50 °C for 1 h. The glass powders were uniaxial pressed and heat treated to form powder compacts. These samples (Glasses 1–3) were heat treated at 850 °C for 10 min, 30 min, 60 min and 90 min and the microstructure was determined by scanning electron microscopy (SEM).

Examination of the phase formation was conducted on the samples (Glasses 1–3) that had been heat treated at 850 °C for 90 min. Therefore, room temperature X-ray diffraction (RT-XRD) measurements were performed.

2.3. Glass analysis

The chemical compositions of the base glasses were analysed using X-ray fluorescence spectroscopy (XRF), ion selective spectroscopy and volumetric titration.

The powder sample was melted into a glass bead in a Pt crucible together with dilithium tetraborate ($Li_2B_4O_7$) in a ratio of 0.8 g:7.2 g. This was accomplished in a fully automatic fluxer (Claisse Fluxy 30, Labortechnik GmbH, Kirchheim, Germany). Two tests were conducted for each sample considered. The XRF analysis was conducted with an XRF unit calibrated according to DIN 51001 (SRS 3000, Siemens AG, Germany). Comparison of the intensities of the fluorescence radiation characteristic to each of the elements present permits the chemical composition of the given sample to be determined.

In order to establish the fluoride content, samples were first melted with soda potash and the melt poured into demineralized water. The pH of the resulting solution was adjusted to 5.0–5.5 using NaOH. The fluoride content was established using ion selective electrodes (Metrohm Ionenmeter 692 and Sampler 730, Deutsche Metrohm GmbH & Co. KG, Germany).

Like the fluoride content, the B_2O_3 content was determined by first melting a mixture of the sample and soda potash and then pouring the melt into deionized water. Subsequently, the solution was brought to the equivalence point where the indicator (methylene red) changed colour using diluted NaOH (or hydrochloric acid). Then the solution was neutralized to pH 7 by 0.1 M NaOH. Following the addition of 5 g mannitol, the solution was again titrated to pH 7. The titration data were then used to calculate the boric oxide content (B_2O_3).

2.4. Measurement techniques

The phase formation and microstructure of the heat treated powder compacts was analysed by means of scanning electron microscopy and room temperature X-ray diffraction investigations.

A diffractometer (D5005, Bruker AXS, Karlsruhe, Germany) with Cu Kα radiation was used to investigate the phase formation. The individual measurements were recorded with a diffraction angle 2Θ from 10° to 60°, at a step size of 0.015° and a step time of 0.5 s. The RT-XRD patterns were interpreted by the evaluation and extrapolation of single measurements (DIFFRAC^{plus}, Bruker AXS). The crystal structure of the investigated crystal phase was calculated with the structural data of Gunawardane et al.[11] by the software ATOMS (V6.1.2, Shape Software, 2004).

The microstructure of the different glass-ceramics and the morphologies of the different types of apatite crystals after one- or two-step heat treatment of the initial glasses was investigated by scanning electron microscopy (LEO DSM 962, Zeiss, Oberkochen, Germany).

3. Results

3.1. Glass analysis and monolithic samples

The X-ray fluorescence spectroscopy analysis of the base glasses in Table 1 showed the chemical compositions.

It was quickly established that the monolithic samples did not show any tendency to crystallize. They did not show any volume crystallization at all. All samples were optically transparent.

3.2. Heat treatment of glass powders

3.2.1. Crystal phase analysis by RT-XRD

The following crystal phases were identified on the basis of room temperature X-ray diffraction analysis of the heat treated Glasses 1–3 with the help of patterns stored in the ICDD database. The pattern of Glass 1 heat treated at 850 °C for 90 min

Table 1
X-ray fluorescence spectroscopy (XRF) analysis of the base glasses

	Glass 1 (wt.%)	Glass 2 (wt.%)	Glass 3 (wt.%)	Error analysis (wt.%)
SiO_2	51.62	52.50	53.09	±0.53
B_2O_3	6.06	5.35	2.69	±0.03
Y_2O_3	11.55	11.93	11.97	±0.07
Al_2O_3	10.56	10.76	10.81	±0.20
CaO	3.34	3.40	3.40	±0.16
Na_2O	7.16	6.93	7.50	±0.17
K_2O	9.32	9.14	10.20	±0.07
F	0.39	–	0.34	±0.02

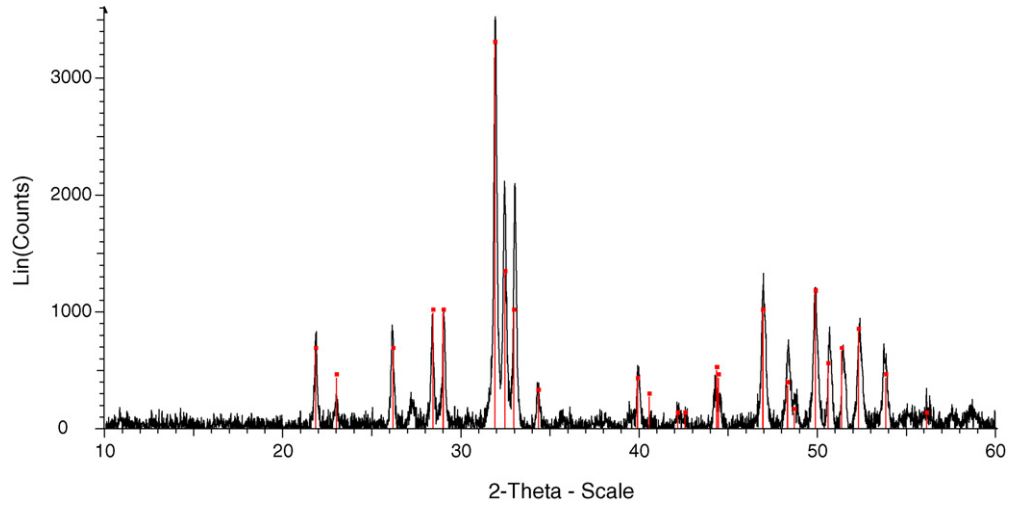

Fig. 1. Room temperature X-ray diffraction pattern of Glass 1 after heat treatment at 850 °C for 90 min.

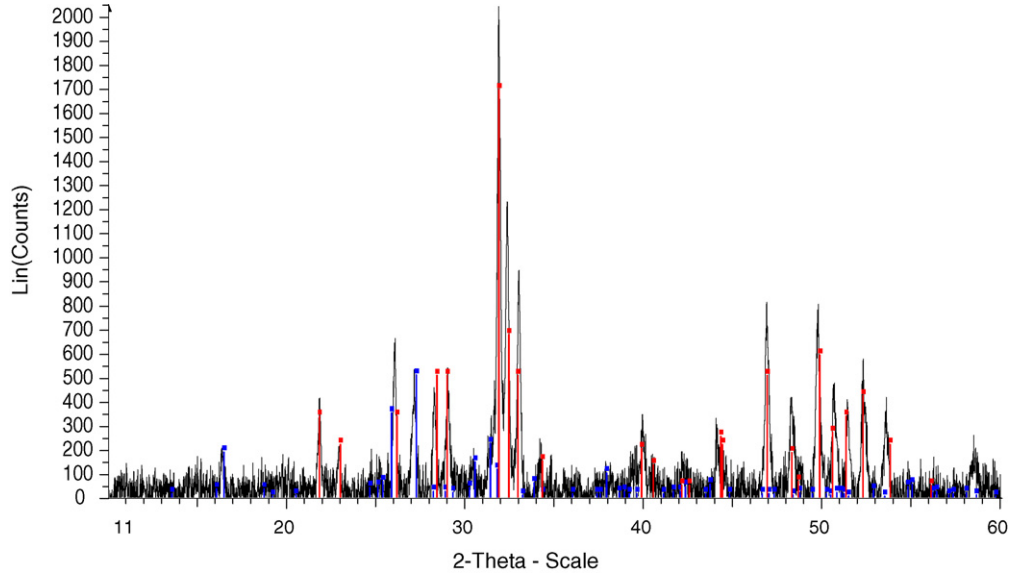

Fig. 2. Room temperature X-ray diffraction pattern of Glass 2 after heat treatment at 850 °C for 90 min.

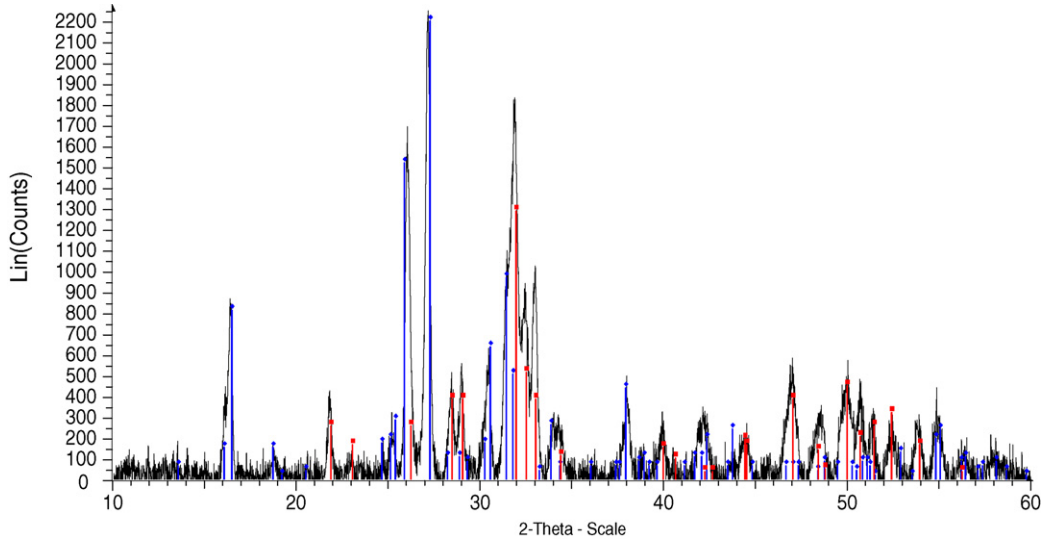

Fig. 3. Room temperature X-ray diffraction pattern of Glass 3 after heat treatment at 850 °C for 90 min.

in Fig. 1 showed the X-ray reflections typical of oxyapatite $NaY_9(SiO_4)_6O_2$ (ICDD 35-0404) and did not show any additional phases. But the patterns of Glasses 2 and 3 in Figs. 2 and 3 heat treated at 850 °C for 90 min exhibited the X-ray reflections of oxyapatite as well as those of leucite ($KAlSi_2O_6$) (ICDD 38-1423) as an additional crystal phase. The base Glasses 1–3 containing fluorine showed after heat treatment the fluorine-free crystal phase oxyapatite $NaY_9(SiO_4)_6O_2$.

In Table 2 the structure data of oxyapatite (Gunawardane et al.[11]) and fluorapatite (Elliot[12]) are compared.

3.2.2. *Microstructure determined by SEM*

Glasses 1–3 heat treated at 850 °C for different times (10 min, 30 min, 60 min and 90 min) all showed the same reaction behaviour (Fig. 4(a–d)). After 10 min of heat treatment, the first glass grains started to crystallize at the surface. The longer the

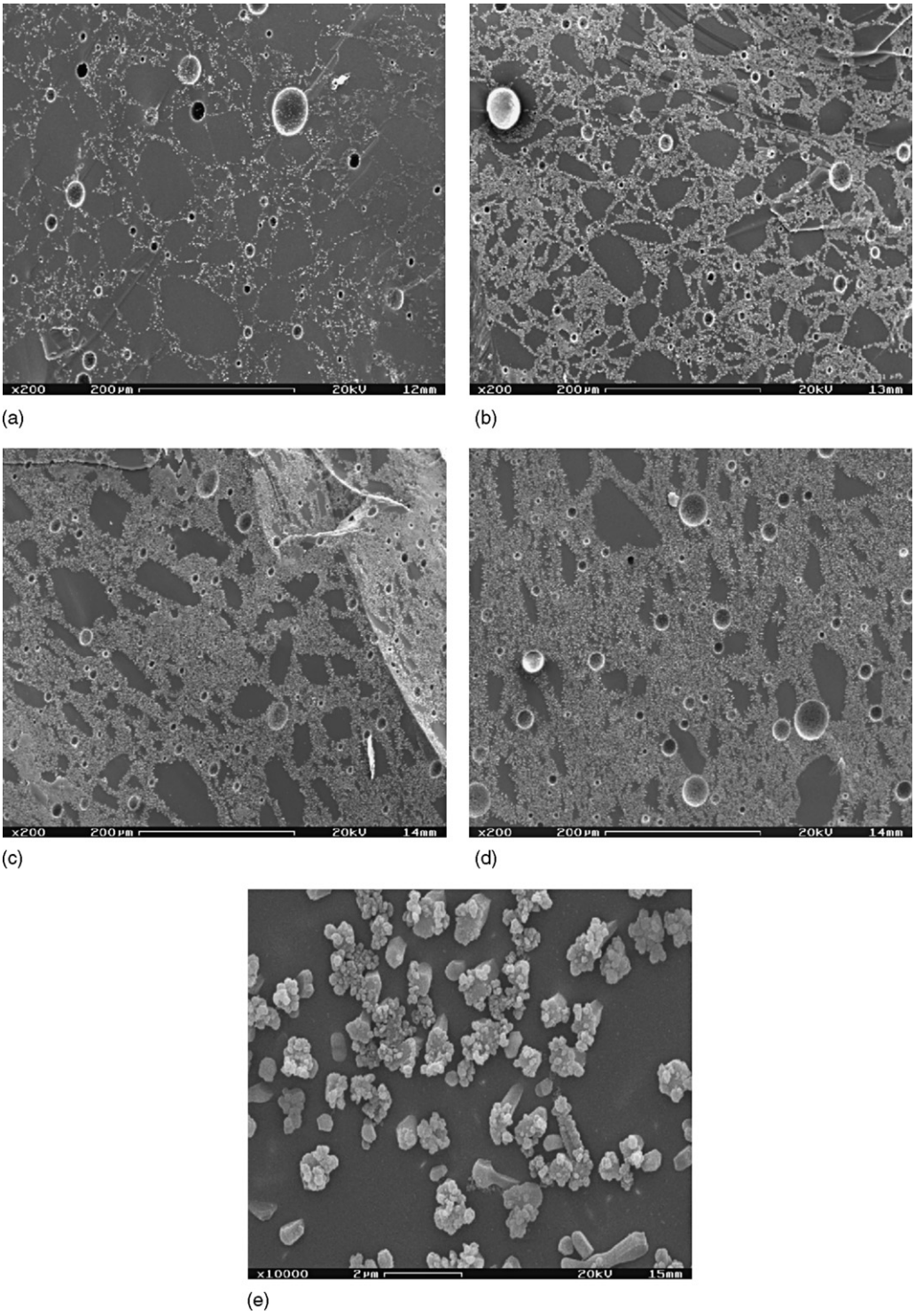

Fig. 4. SEM images of Glass 1 after different times of heat treatment at 850 °C: (a) 10 min, (b) 30 min, (c) 60 min, (d) 90 min and (e) 850 °C/60 min and 1050 °C/30 min.

Table 2
Structural data of $NaY_9(SiO_4)_6O_2$ (Gunawardane et al.[11]) and $Ca_5(PO_4)_3F$ (Elliot[12])

	a-Axis (nm)	*c*-Axis (nm)	Space group
$Ca_5(PO_4)_3F$	0.93718	0.68876	$P6_3/m$
$NaY_9(SiO_4)_6O_2$	0.9334	0.6759	$P6_3/m$

time of thermal treatment lasted, the more glass grains crystallized and a dense crystal belt formed at the surface where ultimately individual grains crystallized completely into the volume.

In addition to the first heat treatment at 850 °C for 1 h, Glass 1 was subjected to a further heat treatment at 1050 °C for 30 min. As shown in Fig. 4(e), the crystals grew and they were more separated, but some of them were aggregated too. Furthermore, instead of being densely packed, the crystals were rather more isolated. The spherical holes on the SEM images were sinter pores.

The glass-ceramics samples had a very high ratio of opacity.

4. Discussion

As presented in Section 1, the nucleation and crystallization mechanism of fluorapatite in SiO_2–Al_2O_3–alkali oxide–earthalkali oxide–P_2O_5–F glasses is based on phase separation processes. This phase separation shows a CaO–F–P_2O_5-rich nanoscaled to microscaled droplet phase in a SiO_2-rich glassy matrix of bulk material. This mechanism is well known and investigated by means of SEM investigations. Crystal phase of $Ca_5(PO_4)_3F$ precipitated either in hexagonal shape of hexagonal needle-like morphology.

In this study we did not see a phase separation by SEM investigations in the bulk of the base glass. Therefore, the classical nucleation sites of apatite were not located in the bulk.

The results of this study show that the crystallization mechanism for the formation of oxyapatite ($NaY_9(SiO_4)_6O_2$) does not involve volume nucleation and crystallization as is the case with fluorapatite, rather it takes place through surface nucleation and crystallization. A very important point of discussion is the reason of the discovered nucleation process. One can assume that the $[SiO_4]^{4-}$ structural units are lower in mobility in comparison to phase separated phosphate groups in dependence of the contend of the non-bridging oxygen (NBO). The different microstructures of these types of oxyapatite base glasses are also a reason for different nucleation centers in comparison to phosphate containing glasses (Fig. 5).

Furthermore, it is possible to control the precipitation of leucite by means of the chemical composition in parallel with

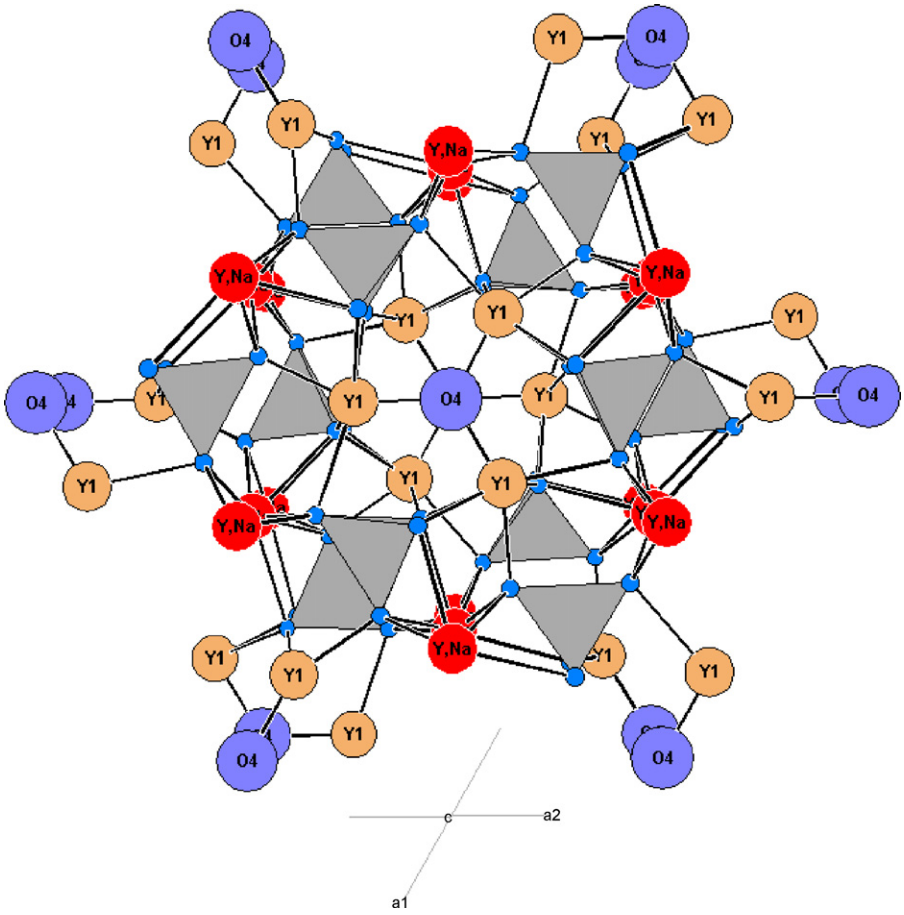

Fig. 5. Crystal structure of the oxyapatite $NaY_9(SiO_4)_6O_2$ calculated with ATOMS V6.1.2 by the crystallographic data of Gunawardane et al.[11] The tetrahedra represent $[SiO_4]^{4-}$ structural units.

the precipitation of oxyapatite. The precipitation of leucite was determined by RT-XRD. That is, a two-fold surface nucleation mechanism was observed.

The amount of B_2O_3 in the base glasses has a decisive influence on the surface crystallization of leucite and its amount. The content of B_2O_3 in Glass 3 (2.69 wt.%) is lower than in Glass 1 (6.06 wt.%) so it is possible that a high B_2O_3 content decreases the precipitation of leucite. Also fluorine seems to have an influence on the precipitation of leucite. Glass 2 does not contain fluorine in comparison to Glass 1 (0.39 wt.%), but it showed leucite as a secondary crystal phase.

In summary, the main result is that the oxyapatite crystallizes from the surface of the grains into the volume. The second main result of this study indicates that a two-fold controlled surface crystallization of oxyapatite and leucite took place in Glasses 2 and 3.

5. Conclusion

We concluded that the formation of oxyapatite proceeds according to the mechanism of controlled surface nucleation and crystallization. Therefore, by using a suitable chemical composition and heat treatment, it is possible to produce glass-ceramics containing oxyapatite crystals. This type of crystal exhibits the similar crystal structure as that of fluorapatite. Therefore, there is an isotype relationship between the two phases: the differences in the crystal structure are found in the structural units, with fluorapatite containing $[PO_4]^{3-}$ and $[F]^{-}$, while oxyapatite containing $[SiO_4]^{4-}$ and $[O]^{2-}$.

Because of its specific optical properties (high opacity), this new glass-ceramic material may be used as a layering material for dental restoration.

References

1. Brömer, H., Deutscher, K., Blencke, B., Pfeil, E. and Strunz, V., Properties of the bioactive implant material 'CERAVITAL'. *Sci. Ceram.*, 1977, **9**, 219–225.
2. Kokubo, T., A/W glass-ceramics: processing and properties. In *An Introduction to Bioceramics*, ed. L. L. Hench and J. Wilson. World Scientific, Singapore, 1993, pp. 75–88.
3. Höland, W., Frank, M. and Schweiger, M., Development of translucent glass-ceramics for dental application. *Glastechn. Ber. Glass Sci. Technol.*, 1994, **67C**, 117–122.
4. Clifford, A. and Hill, R., Apatite–mullite glass-ceramics. *J. Non-Cryst. Solids*, 1996, **196**, 346–351.
5. Moisescu, C., Carl, G. and Rüssel, C., Glass-ceramics with different morphology of fluorapatite crystals. *Phosphorus Res. Bull.*, 1999, **10**, 515–520.
6. Kolitsch, U., Seifert, H. J. and Aldinger, F., The indentity of monoclinic La_2O_3 and monoclinic Pr_2O_3 with $La_{9.33}(SiO_4)_6O_2$ and $Pr_{9.33}(SiO_4)_6O_2$, respectively. *J. Solid State Chem.*, 1995, **120**, 38–42.
7. Ito, J., Silicate apatites and oxyapatites. *Am. Mineral.*, 1968, **53**(May–June), 890–907.
8. Höland, W. and Beall, G. W., *Glass-Ceramic Technology*. The American Ceramic Society, Westerville, 2002.
9. Müller, R., Abu-Hilal, L. A., Reinsch, S. and Höland, W., Coarsening of needle-shaped apatite crystals in $SiO_2{\cdot}Al_2O_3{\cdot}Na_2O{\cdot}K_2O{\cdot}CaO{\cdot}P_2O_5{\cdot}F$ glass. *J. Mater. Sci.*, 1999, **34**, 65–69.
10. van't Hoen, C., Höland, W. and Rheinberger, V., *Glastech. Ber. Glass Sci. Technol.*, 2004, **77C**, 382–386.
11. Gunawardane, R. P., Howie, R. A. and Glasser, F. P., Structure of the oxyapatite $NaY_9(SiO_4)_6O_2$. *Acta Cryst.*, 1982, **B38**, 1564–1566.
12. Elliot, J. C., *Stud. Inorg. Chem.*, 1994, **18**, p64.